Available online at www.sciencedirect.com
SCIENCE DIRECT®
Journal of Sound and Vibration 274 (2004) 985–995
JOURNAL OF SOUND AND VIBRATION
www.elsevier.com/locate/jsvi

# Effect of centrifugal force on natural frequency of lateral vibration of rotating shafts

M. Behzad*, A.R. Bastami

*Mechanical Engineering Department, Sharif University of Technology, P.O. Box 11365-9567, Tehran, Iran*

Received 23 January 2002; accepted 5 June 2003

**Abstract**

This paper investigates the effect of shaft rotation on its natural frequency. Apart from gyroscopic effect, the axial force originated from centrifugal force and the Poisson effect results in change of shaft natural frequency. D'Alembert principle for shaft in cylindrical co-ordinate system, along with the stress–strain relation, gives the non-homogenous linear differential equation, which can be used to calculate axial stress in the shaft. Numerical results of this study show that axial stress produced by shaft rotation has a major effect on the natural frequency of long high-speed shafts, while shaft diameter has no influence on the results. In addition, change in lateral natural frequency due to gyroscopic effect is compared with the results of this study.


## 1. Introduction

Accurate prediction of critical speeds in rotating machinery is of great importance to designers and many attempts have been made to calculate it exactly. Critical speed of a rotating shaft differs from its non-rotating natural frequency. The main reason for this difference is known to be the gyroscopic momentum. Green [1] for the first time studied the effect of gyroscopic momentum on the natural frequency of flexible rotors. Eshleman and Eubanks [2] and Rao [3] have also investigated the effect of gyroscopic momentum on the natural frequency of rotating shafts.

External loading can also change the lateral natural frequency of a rotating shaft. The effect of externally applied axial force and torque on the lateral vibration of shafts has been studied by several researchers. Bokian [4] presented changes in the lateral natural frequency of Euler–Bernoulli beams under axial load with various boundary conditions. Choi et al. [5] derived the

*Corresponding author.
*E-mail addresses:* m_behzad@sina.sharif.ac.ir (M. Behzad), rohani@mehr.sharif.ac.ir (A.R. Bastami).

0022-460X/$ - see front matter © 2003 Elsevier Ltd. All rights reserved.
doi:10.1016/S0022-460X(03)00659-X

equation of motion of a flexible rotating shaft subject to a constant compressive axial load by introducing gyroscopic moments in a consistent manner. Khader [6] studied the stability of a rotating cantilever shaft, carrying a rigid disk at its free end, subjected to follower axial force and torque loads. Chen and Sheu [7] investigated the stability behavior of a rotating Timoshenko shaft with an intermediate attached disk subjected to a longitudinal force analytically. They gave the expressions for frequency equation for various boundary conditions and found critical axial and follower forces numerically. Chen and Ku [8] examined the dynamic stability of a cantilever shaft–disk system subjected to a periodic axial force by the finite element method and gave boundaries of the regions of dynamic instability.

Inertial forces can also induce axial stresses in shafts and beams. Rotation of a beam about an axis perpendicular to the beam axis has also been studied by researchers, in which centrifugal force directly produces axial stress in the beam. Banerjee [9] used dynamic stiffness matrix for Euler–Bernoulli beam with axial force to analyze the vibration of uniform and tapered rotating beams. Lin and Hsiao [10] derived the governing equation for linear vibration of a rotating Timoshenko beam. They included the coupling between extensional and flexural deformation by consistent linearization of the fully geometrically non-linear beam theory and proposed a method based on the power series solution to solve the natural frequency of the rotating Timoshenko beam.

In this paper, a new secondary phenomena which can change the critical speed of shaft is introduced. The change in natural frequency is caused by the axial force, which is generated by rotation of the shaft about its axis. The difference between this phenomena and previous studies is that the shaft rotates about its longitudinal axis, not the transverse axis. Thus, the axial force is not a direct resultant of centrifugal force and it is produced by the Poisson effect. To achieve this goal one needs to first calculate the axial stress distribution in a rotating uniform cylindrical shaft and then evaluate the effect of this force on the lateral natural frequency of the shaft. The method of calculating the governing equations and results are presented in this paper.

## 2. Phenomenon description

Consider a cylindrical shaft with inner radius $a$, outer radius $b$ and length $L$, which rotates with a constant rotational speed $\Omega$ as shown in Fig. 1. The shaft is supported on two bearings at shaft ends, which suppress axial movement of the shaft.

Shaft rotation produces a centrifugal force that creates a radial stress in the shaft. It is well known that because of the Poisson effect, normal stresses in one direction produce normal strain in the lateral direction. If the strain in the lateral direction is forced to zero a normal stress in that

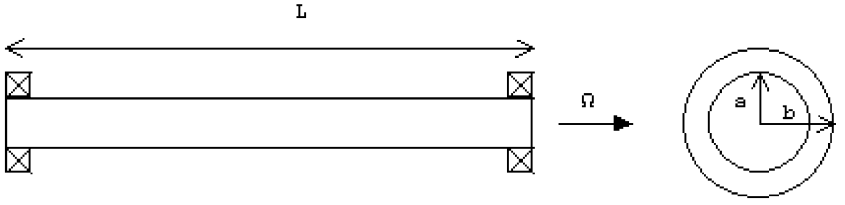


Fig. 1. Shaft dimension.

direction will be created in order to compensate the strain. Similarly, the radial stress in the rotating shaft creates axial stress in the shaft. The sum of the axial stresses on the cross-section of the shaft produces a net axial force in it. The existence of axial force changes the natural frequency of lateral vibration of the shaft. Hence, in this manner shaft rotation can change its natural frequencies.

In the following sections by solving governing elasticity equations, axial stress in the shaft is found and then the natural frequency change due to this axial force will be computed.

## 3. Calculation of axial force in the rotating shaft

For calculating the axial force that is produced as a result of shaft rotation, the 3-D linear elasticity relations are used. An axisymmetric shaft with a length much larger than its diameter is considered in this study. A plane strain problem is assumed because the bearings suppress axial movement of the shaft.

The cylindrical co-ordinate system, in which the $Z$-axis is coincident with the shaft axis of rotation, is used in this research. Displacement in the directions of $r$, $\theta$ and $z$ are, respectively, shown by $u$, $v$ and $w$. Due to D'Alembert principle, the shaft can be considered stationary and the inertia force of $r\Omega^2\,\mathrm{d}m$, originating from centrifugal acceleration, is applied in the radial direction. In this case the equilibrium equation for the shaft in radial direction is as follows:

$$\frac{\partial}{\partial r}(r\sigma_r) - \sigma_\theta = -\rho r^2 \Omega^2, \tag{1}$$

where $\sigma_r$ and $\sigma_\theta$ are the radial and circumferential stresses, $\rho$ is the shaft density and $\Omega$ is the constant shaft speed. The stress–strain relations for plain strain are as follows [11]:

$$\begin{aligned}
\sigma_r &= \frac{E}{(1+v)(1-2v)}(v\varepsilon_\theta + (1-v)\varepsilon_r),\\
\sigma_\theta &= \frac{E}{(1+v)(1-2v)}(v\varepsilon_r + (1-v)\varepsilon_\theta),\\
\sigma_z &= \frac{E}{(1+v)(1-2v)}(v\varepsilon_\theta + v\varepsilon_r),
\end{aligned} \tag{2}$$

where $\sigma$, $\varepsilon$, $E$ and $v$ are, respectively, stress, strain, Young's modulus of elasticity and the Poisson ratio. In accordance with axisymmetry and plain strain assumption, the $v$ and $w$ components of displacement are zero and the strain–displacement relations can be written as [11]

$$\begin{aligned}
\varepsilon_r &= \frac{\mathrm{d}u}{\mathrm{d}r},\\
\varepsilon_\theta &= \frac{u}{r}.
\end{aligned} \tag{3}$$

Substituting relations (2) and (3) into Eq. (1), the equilibrium equation is restated in terms of only $u$ displacement component:

$$r^2\frac{\mathrm{d}^2u}{\mathrm{d}r^2} + r\frac{\mathrm{d}u}{\mathrm{d}r} - u = -\frac{(1+v)(1-2v)}{E(1-v)}\rho\Omega^2 r^3. \tag{4}$$

Eq. (4) is a second order linear non-homogenous differential equation and can be solved by calculating homogenous and particular answers separately. The homogenous answer can be written in the following form:

$$u_h = r^{\alpha}, \tag{5}$$

where $\alpha$ can be found by substituting Eq. (5) into the homogenous form of Eq. (4), as follows:

$$\alpha(\alpha - 1) + (\alpha - 1) = 0 \Rightarrow \alpha = \pm 1. \tag{6}$$

The homogenous answer with two constants $c_1$ and $c_2$ becomes

$$u_h = c_1 r + \frac{c_2}{r}. \tag{7}$$

Assuming $cr^3$ for the particular answer and substituting into Eq. (4) gives

$$u_p = -\frac{1}{8}\frac{(1+\nu)(1-2\nu)}{E(1-\nu)}\rho\Omega^2 r^3. \tag{8}$$

The complete answer for Eq. (4) now can be written in the following form:

$$u = u_h + u_p = c_1 r + \frac{c_2}{r} - \frac{1}{8}\frac{(1+\nu)(1-2\nu)}{E(1-\nu)}\rho\Omega^2 r^3. \tag{9}$$

The coefficients $c_1$ and $c_2$ can be determined from boundary conditions. There are two boundary conditions at the inner surface ($r = a$) and the outer surface ($r = b$) of the shaft. These boundary conditions state that radial stresses at free surfaces are zero, which can be restated in terms of radial displacement $u$ by relations (2) and (3). Applying these boundary conditions, coefficients $c_1$ and $c_2$ will be calculated as follows:

$$\begin{aligned} c_1 &= \frac{(1-2\nu)(3-2\nu)(1+\nu)}{8E(1-\nu)}\rho\Omega^2(a^2+b^2), \\ c_2 &= \frac{(3-2\nu)(1+\nu)}{8E(1-\nu)}\rho\Omega^2 a^2 b^2. \end{aligned} \tag{10}$$

By substituting the $c_1$ and $c_2$ values into Eq. (9), the displacement field $u$ can be calculated. For a solid shaft having zero inner radius ($a = 0$), the boundary condition at the inner surface does not exist anymore and instead the condition of finite stress at $r = 0$ must be used. This means that coefficient $c_2$ in Eq. (9) must be zero and this condition is satisfied by the values given in Eq. (10). Therefore, the same answer as the case of a hollow shaft is valid for a solid shaft and the following results are valid for solid shafts as well as hollow shafts.

Axial stress in the shaft can be found by substituting displacement $u$ into relations (2) and (3) as follows:

$$\sigma_z = \frac{\nu}{4(1-\nu)}[(3-2\nu)(a^2+b^2) - 2r^2]\rho\Omega^2. \tag{11}$$

The net axial force in the cross-section of shaft, $P$, is the integral of axial stress on the section of the shaft:

$$P = \int_a^b 2\pi r\sigma_z \, \mathrm{d}r. \tag{12}$$

By substituting $\sigma_z$ from Eq. (11) into Eq. (12), one has

$$P = \frac{\pi}{2} v\rho\Omega^2(b^4 - a^4). \tag{13}$$

For a shaft with circular cross-section, the polar moment of inertia is $I_p = (\pi/2)(b^4 - a^4)$; hence, Eq. (13) can be rewritten in the following form:

$$P = v\rho I_p \Omega^2. \tag{14}$$

Eq. (14) gives the resulting axial force in a rotating shaft. As can be seen in Eq. (14), the axial force is proportional to the Poisson ratio and vanishes if the Poisson ratio is zero. This confirms that axial force is produced as a result of the Poisson phenomenon. Axial force is also proportional to the square of the shaft speed. This shows that increasing the shaft speed has a great effect on axial force.

## 4. Change in natural frequency of lateral vibration

Existence of the axial force in the shaft changes its equation of lateral vibration. The equation of lateral vibration of Euler–Bernoulli beam in the presence of axial force $P$ can be written as [12]

$$EI\frac{\mathrm{d}^4 y}{\mathrm{d}x^4} - P\frac{\mathrm{d}^2 y}{\mathrm{d}x^2} - \rho A\omega^2 y = 0, \tag{15}$$

where $A$ and $I$ are area and second moment of area of shaft cross-section, respectively. Since rotary inertia is neglected in Euler–Bernoulli beam theory, Eq. (15) is also valid for a rotating beam. One can solve this equation with specified boundary conditions and calculate natural frequencies as eigenvalues of the equation. For a shaft with two short bearings at ends, the simply supported boundary condition can be used. It can be shown that the first eigenvalue of Eq. (15) is given by [13]

$$\omega^2 = \frac{\pi^2 EI_d}{\rho AL^2}\left(\frac{\pi^2}{L^2} + \frac{P}{EI_d}\right). \tag{16}$$

Substituting axial force $P$, from Eq. (14) into Eq. (16) gives

$$\omega^2 = \frac{\pi^2 EI_d}{\rho AL^2}\left(\frac{\pi^2}{L^2} + \frac{v\rho I_p\Omega^2}{EI_d}\right). \tag{17}$$

Assuming $I_p/I_d = 2$, which is valid for circular cross-sections, Eq. (17) becomes

$$\frac{\omega^2 - \omega_0^2}{\omega_0^2} = \frac{2v\rho}{\pi^2 E} L^2\Omega^2, \tag{18}$$

where $\omega_0$ is the first natural frequency of the non-rotating shaft. Eq. (18) shows a relative change in the natural frequency of the rotating shaft in terms of shaft parameters. Three groups of parameters affecting the natural frequency are: physical properties of the material ($v\rho/E$), geometrical dimension of the shaft ($L^2$), and shaft rotation speed ($\Omega^2$). It is notable that among geometrical dimensions of shaft only length appears in Eq. (18) and diameter has no effect on natural frequency change. Although this is only shown for a simply supported shaft, it can be

proved in general for all boundary conditions that the ratio of eigenvalues of eigenproblem (15) for two different rotation speeds is independent of shaft diameter.

In order to expand the application of this theory to other boundary conditions, it is necessary to eliminate axial freedom at boundaries. Hence, the possible boundary conditions are pin and clamp supports, and free ends cannot be used. For a clamp–clamp shaft or clamp–pin shaft the natural frequency cannot be written in closed form such as Eq. (17). But it can be calculated by numerical methods. The transfer matrix method, which is an accepted method in rotordynamics [3,14], is used in the subsequent sections to calculate the natural frequency of a shaft subjected to axial force for other boundary conditions. The applied transfer matrix method considers continuous shaft modelling [15] which leads to exact results.

## 5. Comparison with gyroscopic effect

The equation of lateral vibration of a rotating shaft considering rotary inertia and gyroscopic momentum is as follows [16]:

$$EI\frac{\mathrm{d}^4y}{\mathrm{d}x^4} - \rho I\omega(2\Omega - \omega)\frac{\mathrm{d}^2y}{\mathrm{d}x^2} - \rho A\omega^2 y = 0. \tag{19}$$

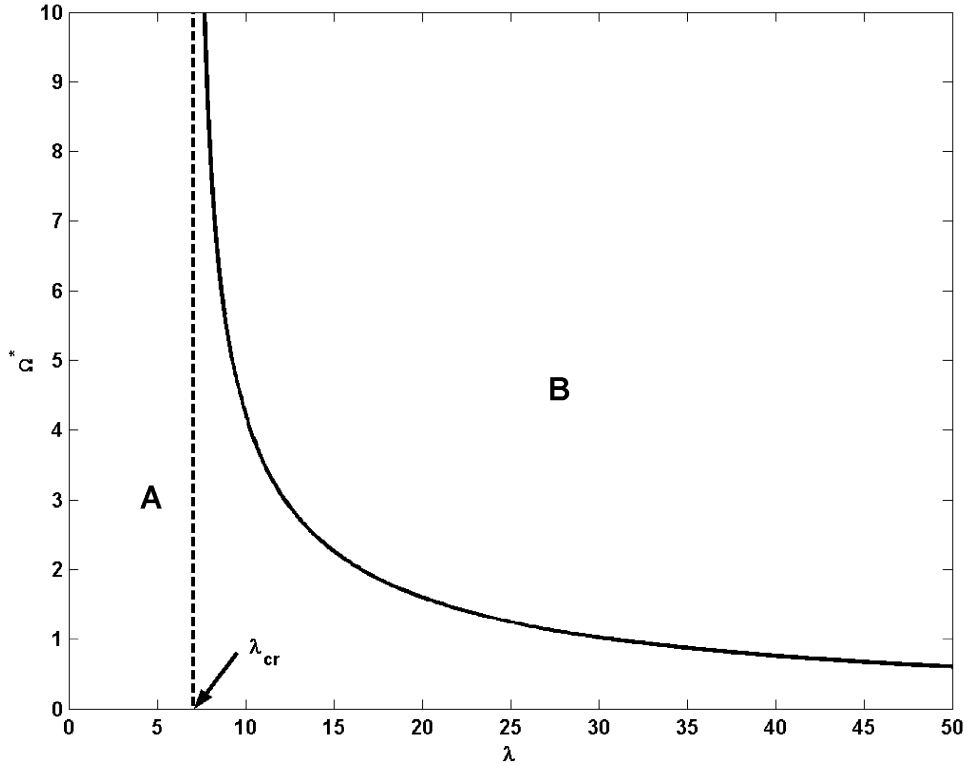


Fig. 2. Comparison of gyroscopic effect and effect of axial force induced by rotation for pin–pin shaft. Region A: gyroscopic effect is predominant; region B: axial force induced by rotation is predominant.

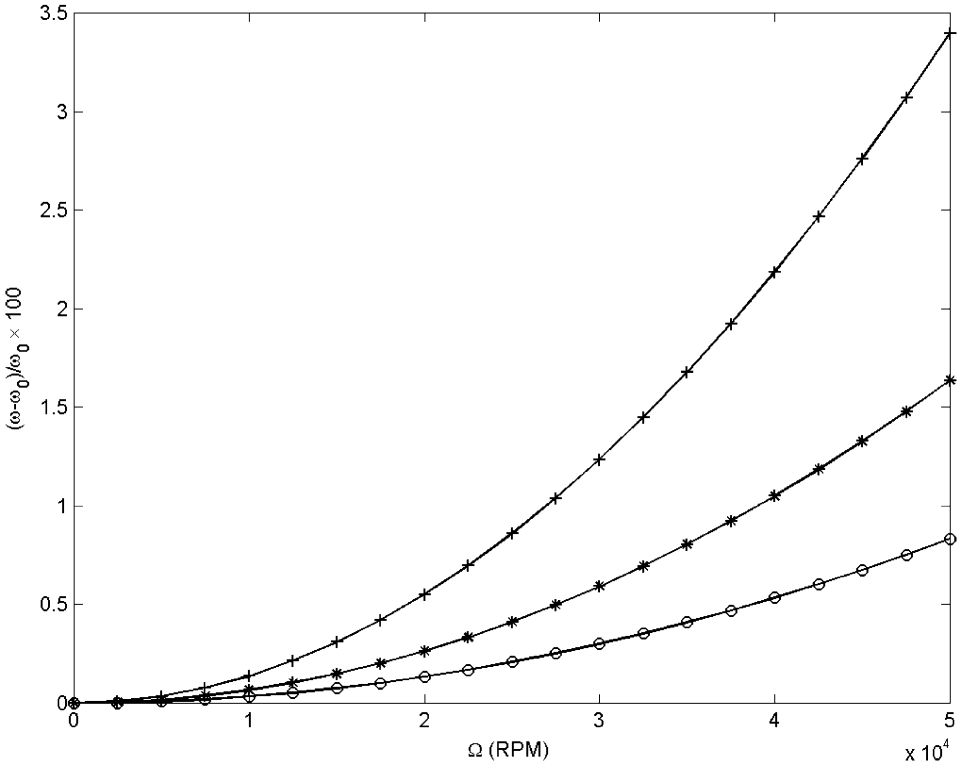


Fig. 3. Relative change of natural frequency versus shaft speed with different boundary conditions and 1-m length: $-+-$, pin–pin; $-*-$ pin–clamp; $-\bigcirc-$, clamp–clamp.

The first eigenvalue of Eq. (19) considering pin–pin boundary conditions is given by [16]

$$\omega = \frac{\frac{I}{A}\frac{\pi^2}{L^2}\Omega \pm \sqrt{\left(\frac{I}{A}\frac{\pi^2}{L^2}\Omega\right)^2 + \frac{EI}{\rho A}\left(1+\frac{I}{A}\frac{\pi^2}{L^2}\right)\frac{\pi^4}{L^4}}}{1+\frac{I}{A}\frac{\pi^2}{L^2}}. \tag{20}$$

The positive root represents the frequency of a forward whirling mode which is greater than the non-rotating shaft natural frequency, while the negative root represents the frequency of a backward whirling mode which is smaller than non-rotating shaft natural frequency. Forward whirl is more common in practice and will be considered in the following. Change in the natural frequency according to gyroscopic effect can be written in the following form:

$$\frac{\omega^2-\omega_0^2}{\omega_0^2} = 2s + 2\sqrt{s^2+s}, \tag{21}$$

where $s$ is a dimensionless parameter defined as $s = (\rho/E)(IL^2/(AL^2+I\pi^2))\Omega^2$. Eqs. (18) and (21) can be used to compare the effect of axial force induced by rotation and gyroscopic momentum on

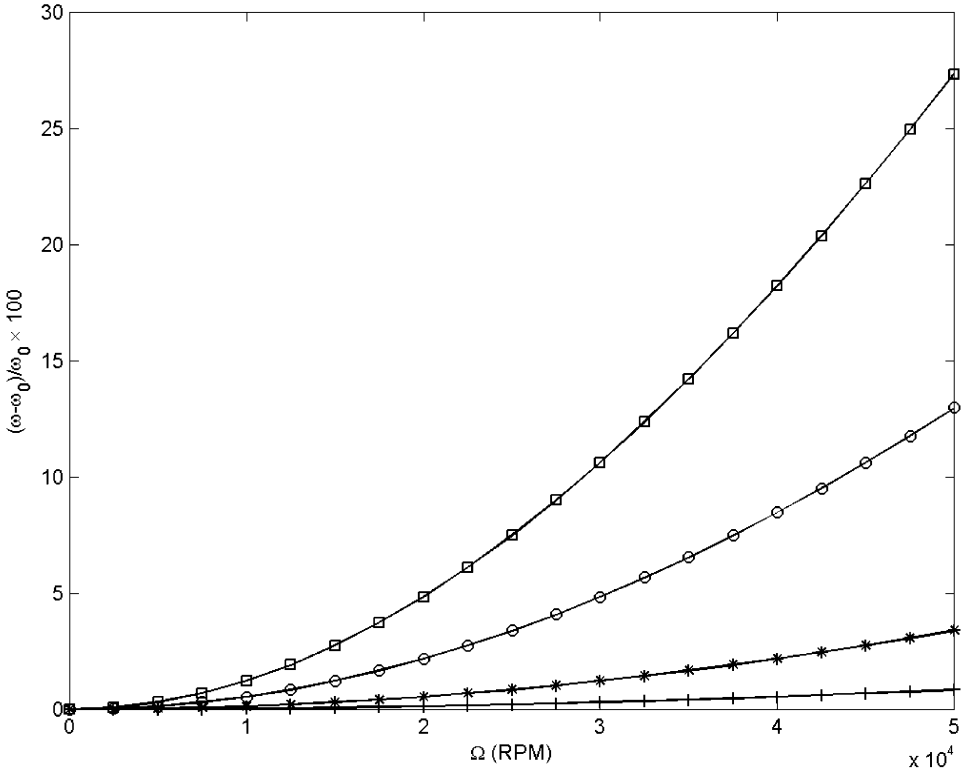


Fig. 4. Relative change of natural frequency versus shaft speed for a pin–pin steel shaft: $-+-$, $L = 0.5$ m; $-*-$, $L = 1$ m; $-\bigcirc-$, $L = 2$ m; $-\square-$, $L = 3$ m.

the natural frequency of rotating shafts. Comparing Eqs. (18) and (21) one obtains

$$\left(\frac{v^2}{\pi^4}\lambda^2 - \frac{v(2-v)}{\pi^2}\right) = \frac{1}{\Omega^{*2}}, \tag{22}$$

where $\lambda = \sqrt{A/I}L$ and $\Omega^* = \sqrt{\rho/E}L\Omega$ are dimensionless slenderness ratio and rotational speeds, respectively. Assuming $v = 0.33$, $\Omega^*$ is plotted versus $\lambda$ in Fig. 2. This graph shows two regions namely: A in which the gyroscopic effect is predominant and B where the effect of axial force induced by shaft rotation is more important. It can be seen in Fig. 2 that there is a critical slenderness ratio $\lambda_{cr}$, where for $\lambda \leqslant \lambda_{cr}$, the gyroscopic effect always has more considerable effect, while for $\lambda > \lambda_{cr}$ the plotted curve is the boundary of regions A and B where for shaft speeds greater than the curve value, the axial force will have a major role. Therefore, the effect of axial force is more important than the gyroscopic effect in slender and high-speed shafts.

In general, gyroscopic effect is significant when heavy disks are mounted on the shaft, but the amount of axial force produced in the shaft is independent of the existence of disks. Therefore, in long power transmission shafts, without any heavy disk and operating at high speeds the effect of axial force induced by shaft rotation is more important than the gyroscopic effect.

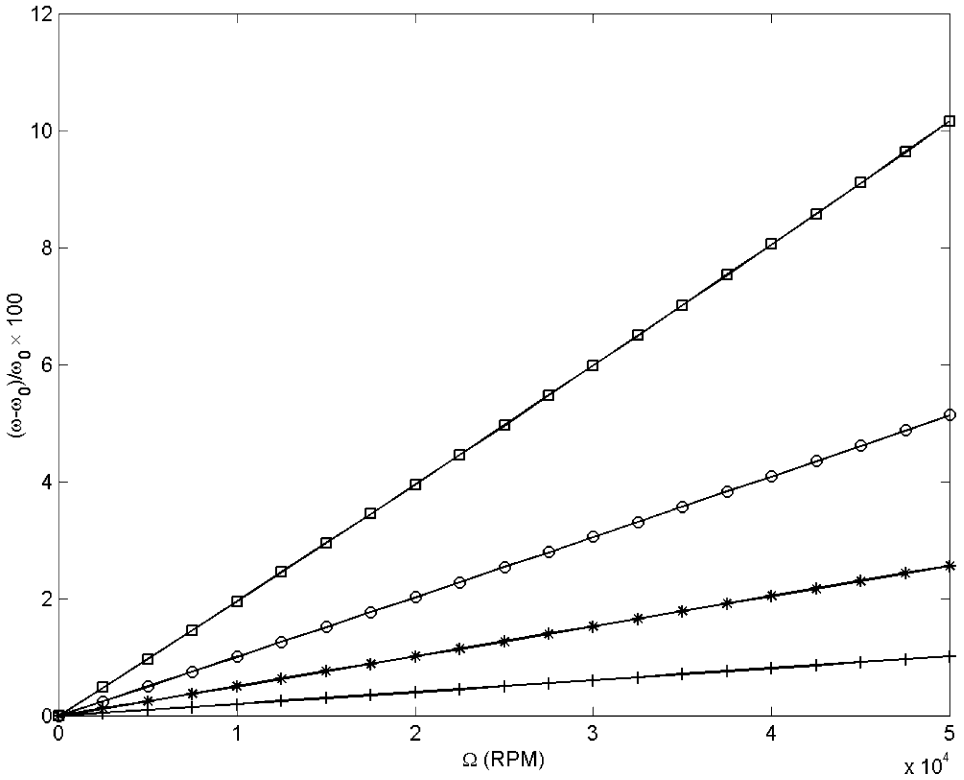


Fig. 5. Relative change of natural frequency versus shaft speed for a pin–pin steel shaft due to gyroscopic effect: $-+-$, $r = 0.02$ m; $-*-$, $r = 0.05$ m; $-\bigcirc-$, $r = 0.1$ m; $-\square-$, $r = 0.2$ m.

## 6. Numerical results

As seen in the previous section, the ratio of lateral natural frequency of rotating shaft to non-rotating shaft for a specific boundary condition is a function of material properties, geometrical dimension (length only) and shaft speed. For numerical investigations, the shaft material is assumed to be steel with: $E = 2.07 \times 10^{11}$ Pa, $v = 0.33$ and $\rho = 7800$ kg/m$^3$. In Fig. 3, percent of relative change in the natural frequency, $(\omega - \omega_0)/\omega_0 \times 100$, caused by the axial force is plotted versus shaft speed for three different boundary conditions including pin–pin, pin–clamp and clamp–clamp. Results are obtained for a shaft of 1 m length. It can be seen that for a pin–pin boundary condition, a relative change in the natural frequency is more than other boundary conditions.

Fig. 4 shows the effect of shaft length on the relative change in natural frequency. It can be concluded that increasing the shaft length will increase $(\omega - \omega_0)/\omega_0 \times 100$ up to nearly 30% for a 3-m shaft at 50 000 r.p.m. The presented graphs are valid for any shaft diameter.

As mentioned previously, gyroscopic momentum also changes the lateral natural frequency of rotating shafts. Fig. 5 is presented for comparing gyroscopic effect with the effect of axial force induced by rotation. In this figure, percent of relative change in natural frequency, $(\omega - \omega_0)/\omega_0 \times 100$, caused by gyroscopic momentum versus shaft speed is plotted according to Eq. (21). The

shaft length in Fig. 5 is 1 m and various graphs are plotted for different shaft diameters. It can be seen from Fig. 5 that gyroscopic momentum in thick shafts has greater effect than in thin shafts.

## 7. Conclusions

It has been shown as to how the rotation of a cylindrical shaft can affect its lateral natural frequency except gyroscopic momentum. This phenomenon is a direct result of the Poisson effect while shaft axial movement is prevented.

For long shafts at high rotational speed this effect is considerable, but for ordinary shafts with normal rotational speed it is negligible. Comparing the results for different boundary conditions shows that this phenomenon in a simply supported shaft is more important than other boundary conditions. An interesting result is that the shaft diameter has no influence on a relative change of the natural frequency.

A comparison with gyroscopic momentum shows that a change in the natural frequency by both phenomena have the same order of magnitude and depending on shaft dimension and speed one may become greater.

## Appendix. Nomenclature

| | |
|---|---|
| $a$ | shaft inner radius |
| $b$ | shaft outer radius |
| $c_1$, $c_2$ | arbitrary constants |
| $E$ | Young's modulus |
| $L$ | shaft length |
| $P$ | axial force |
| $r$, $\theta$, $z$ | cylindrical co-ordinates |
| $u$, $v$, $w$ | displacement in radial, circumferential and axial direction |
| $\varepsilon$ | strain |
| $\lambda$ | slenderness ratio |
| $\nu$ | the Poisson ratio |
| $\rho$ | density |
| $\sigma$ | stress |
| $\omega$ | natural frequency of shaft |
| $\omega_0$ | natural frequency of non-rotating shaft |
| $\Omega$ | shaft rotation speed |
| $\Omega^*$ | dimensionless shaft rotation speed |

## References

[1] R.B. Green, Gyroscopic effects on the critical speeds of flexible rotors, *Transactions of the American Society of Mechanical Engineers* 70 (1948) 369–376.

[2] R.L. Eshleman, R.A. Eubanks, On the critical speeds of a continuous shaft–disk system, *Journal of Engineering for Industry, Transactions of the American Society of Mechanical Engineers* 80 (4) (1967) 645–652.

[3] S.S. Rao, *Rotor Dynamics*, Wiley, New York, 1983.
[4] A. Bokian, Natural frequencies of beams under compressive axial loads, *Journal of Sound and Vibration* 126 (1) (1988) 49–65.
[5] S.H. Choi, C. Pierre, A.G. Ulsoy, Consistent modeling of rotating Timoshenko shafts subject to axial loads, *Journal of Vibration and Acoustics, Transactions of the American Society of Mechanical Engineers* 114 (1992) 249.
[6] N. Khader, Stability of rotating shafts loaded by follower axial force and torque load, *Journal of Sound and Vibration* 182 (5) (1995) 759–773.
[7] L.W. Chen, H.C. Sheu, Stability behavior of a shaft–disk system subjected to longitudinal force, *Journal of Propulsion and Power* 14 (3) (1998) 375–383.
[8] L.W. Chen, D.M. Ku, Dynamic stability of a cantilever shaft–disk system, *Journal of Vibration and Acoustics, Transactions of the American Society of Mechanical Engineers* 114 (1992) 326–329.
[9] J.R. Banerjee, Free vibration of centrifugally stiffened uniform and tapered beams using the dynamic stiffness method, *Journal of Sound and Vibration* 233 (5) (2000) 857–875.
[10] S.C. Lin, K.M. Hsiao, Vibration analysis of a rotating Timoshenko beam, *Journal of Sound and Vibration* 240 (2) (2001) 303–322.
[11] S.P. Timoshenko, J.N. Goodier, *Theory of Elasticity*, 3rd Edition, McGraw-Hill, New York, 1970.
[12] S.P. Timoshenko, D.H. Young, W. Weaver, *Vibration Problems in Engineering*, 4th Edition, Wiley, New York, 1974.
[13] S.S. Rao, *Mechanical Vibration*, 3rd Edition, Addison-Wesley, New York, 1995.
[14] E.C. Pestel, F.A. Leckie, *Matrix Methods in Elastomechanics*, McGraw-Hill, New York, 1963.
[15] N.F. Rieger, S. Zhou, Development and verification of transfer matrix unbalance response procedure for three-level rotor-foundation systems, *Journal of Vibration and Acoustics, Transactions of the American Society of Mechanical Engineers* 120 (1998) 240–251.
[16] T. Yamamoto, Y. Ishida, *Linear and Nonlinear Rotordynamics: A Modern Treatment with Applications*, Wiley, New York, 2001.